

# Spectral Structure of Electron Antineutrinos from Nuclear Reactors

D. A. Dwyer\*

*Lawrence Berkeley National Laboratory, Berkeley, CA, USA*

T. J. Langford†

*Yale University, New Haven, CT, USA*

(Dated: October 3, 2018)

Recent measurements of the positron energy spectrum obtained from inverse beta decay interactions of reactor electron antineutrinos show an excess in the 4 to 6 MeV region relative to current predictions. First-principle calculations of fission and beta decay processes within a typical pressurized water reactor core identify prominent fission daughter isotopes as a possible origin for this excess. These calculations also predict percent-level substructure in the antineutrino spectrum due to Coulomb effects in beta decay. Precise measurement of this substructure can constrain nuclear reactor physics. The substructure can be a systematic uncertainty for measurements utilizing the detailed spectral shape.

PACS numbers: 14.60.Pq, 14.60.Lm, 28.41.-i, 23.40.-s, 25.85.-w

Keywords: neutrino, reactor, Daya Bay, RENO, Double CHOOZ, hierarchy

## INTRODUCTION

Determination of the mixing angle  $\theta_{13}$  required a new generation of reactor antineutrino experiments with unprecedented statistical precision [1–3]. The Daya Bay and RENO experiments have each detected  $\sim 10^6$  reactor  $\bar{\nu}_e$  interactions [4, 5]. Proper characterization of the  $\bar{\nu}_e$  energy spectrum emitted by nuclear reactors is important for such measurements of neutrino properties. The standard method of modeling the  $\bar{\nu}_e$  emission by nuclear reactors relies on the correlation between the energy spectra of the  $\beta^-$  and  $\bar{\nu}_e$  in beta decay. Here we refer to this method as  $\beta^-$  conversion. For a single beta decay, the prediction of the  $\bar{\nu}_e$  spectrum from the measured  $\beta^-$  spectrum can be done with high precision. In the 1980's, foils of the fissile isotopes  $^{235}\text{U}$ ,  $^{239}\text{Pu}$ , and  $^{241}\text{Pu}$  were exposed to a thermal neutron flux from the ILL reactor, and the cumulative beta decay  $\beta^-$  spectra of the fission daughters were measured [6–8]. More recently, a similar measurement was made for  $^{238}\text{U}$  [9]. The fission of four main parent isotopes represent  $>99\%$  of reactor  $\bar{\nu}_e$  emission. Given that each measured  $\beta^-$  spectrum is composed of thousands of unique beta decays, the conversion must be done en masse. This introduces uncertainties of a few percent in the corresponding prediction of the cumulative  $\bar{\nu}_e$  spectra. Detailed descriptions of such calculations can be found in [10–12]. A recent study suggested that the uncertainties in conversion of the  $\beta^-$  to  $\bar{\nu}_e$  spectrum may have been underestimated due to shape corrections for forbidden beta decays [13].

In this note we discuss an alternative calculation of  $\bar{\nu}_e$  emission by nuclear reactors based on nuclear databases. This *ab initio* approach relies on direct estimation of the  $\bar{\nu}_e$  spectrum from the existing surveys of nuclear data. This method suffers from rather large uncertainties in our knowledge of the fission and decay of the  $>1000$  isotopes

predicted to be present in a nuclear reactor core. Despite these uncertainties, the *ab initio* calculation predicts a spectral bump with  $E_{\bar{\nu}}=5\text{--}7$  MeV ( $E_{e^+}=4\text{--}6$  MeV) relative to the  $\beta^-$  conversion method. Recent measurements of the positron energy spectra from  $\bar{\nu}_e$  inverse beta decay ( $\bar{\nu}_e + p \rightarrow e^+ + n$ ) show a similar  $\sim 10\%$  excess of positrons detected with energies from 4 to 6 MeV. We also observe substructure at the level of a few percent in the calculated energy spectra, which is difficult to demonstrate from the  $\beta^-$  conversion method. This substructure is due to discontinuities introduced by the Coulomb phase space correction in the  $\bar{\nu}_e$  spectrum of each unique decay branch. Precise measurement of this substructure could provide a unique handle on the nuclear physics occurring within a reactor. When not predicted in the model, the substructure may present a systematic uncertainty for measurements relying on high-resolution features of the reactor  $\bar{\nu}_e$  energy spectrum, for example [14, 15].

## CALCULATION OF THE $\bar{\nu}_e$ SPECTRUM

The *ab initio* method of calculating the  $\bar{\nu}_e$  spectrum follows that presented in [13, 16]. Considering a reactor operating at equilibrium, the total antineutrino spectrum can be estimated as the sum of a large number of beta decay spectra,

$$S(E_{\bar{\nu}}) = \sum_{i=0}^n R_i \sum_{j=0}^m f_{ij} S_{ij}(E_{\bar{\nu}}). \quad (1)$$

The equilibrium decay rate of isotope  $i$  in the reactor core is  $R_i$ . The isotope decays to a particular energy level  $j$  of the daughter isotope with a relative probability, or branching fraction,  $f_{ij}$ . The antineutrino spectrum for each decay branch is given by  $S_{ij}(E_{\bar{\nu}})$ . The collective  $\bar{\nu}_e$

emission from a reactor is due to  $>1000$  daughter isotopes with  $>6000$  unique beta decays.

Estimation of the decay rates  $R_i$  depend on our knowledge of the nuclear processes within the reactor core. For a fission of a parent nucleus,  ${}^A_Z N_p$ , the probability of fragmenting to a particular daughter nucleus  ${}^{A'}_Z N_d$  is given by the *instantaneous* yield,  $Y_{pd}^i$ . The majority of these fission daughters are unstable, and will decay until reaching a stable isotopic state. The *cumulative* yield  $Y_{pi}^c$  is the probability that a particular isotope  ${}^{A'}_Z N_i$  is produced via the decay chain of any initial fission daughter. On average, the daughter isotopes of each fission undergo 6 beta decays until reaching stability. For short-lived isotopes, the decay rate  $R_i$  is approximately equal to the fission rate  $R_p^f$  of the parent isotope  $p$  times the cumulative yield of the isotope  $i$ ,

$$R_i \simeq \sum_{p=0}^P R_p^f Y_{pi}^c \quad (2)$$

The ENDF/B.VII.1 compiled nuclear data contains tables of the cumulative fission yields of 1325 fission daughter isotopes, including relevant nuclear isomers [17, 18]. Evaluated nuclear structure data files (ENSDF) provide tables of known beta decay endpoint energies and branching fractions for many isotopes [19]. Over 4000 beta decay branches are found which have endpoints above the 1.8 MeV threshold for inverse beta decay. The spectrum of each beta decay  $S_{ij}(E_{\bar{\nu}})$  was calculated including Coulomb [20], radiative [21], finite nuclear size, and weak magnetism corrections [13]. In the following calculations we begin by assuming that all decays have allowed Gamow-Teller spectral shapes. The impact of forbidden shape corrections will be discussed later in the text.

The upper panel of Fig. 1 shows the electron spectrum per fission of  ${}^{235}\text{U}$  calculated according to Eq. 1. The  $\beta^-$  spectrum measured in the 1980s using the BILL spectrometer is shown for comparison [6]. Both spectra are absolutely normalized in units of electrons per MeV per fission. The lower panel shows the calculated  $\bar{\nu}_e$  spectrum for a nominal nuclear reactor with relative fission rates of 0.584, 0.076, 0.29, 0.05 respectively for the parents  ${}^{235}\text{U}$ ,  ${}^{238}\text{U}$ ,  ${}^{239}\text{Pu}$ ,  ${}^{241}\text{Pu}$ . The spectra have been weighted by the cross section for inverse beta decay to more closely correspond to the spectra observed by experiments. Prediction of the  $\bar{\nu}_e$  spectrum by  $\beta^-$  conversion of the BILL measurements [11, 12] shows a different spectral shape. In particular, there is a bump near 6 MeV in the calculated spectrum not shown by the  $\beta^-$  conversion method. Note that the hybrid approach of Ref. [11] used the *ab initio* calculation to predict most of the  $\beta^-$  and  $\bar{\nu}_e$  spectra, but additional fictional  $\beta^-$  branches were added so that the overall electron spectra would match the BILL measurements. These corresponding  $\bar{\nu}_e$  spectra for these branches were estimated using the  $\beta^-$  conversion method. Since this method is constrained to match

the BILL measurements, it is grouped with the other  $\beta^-$  conversion predictions.

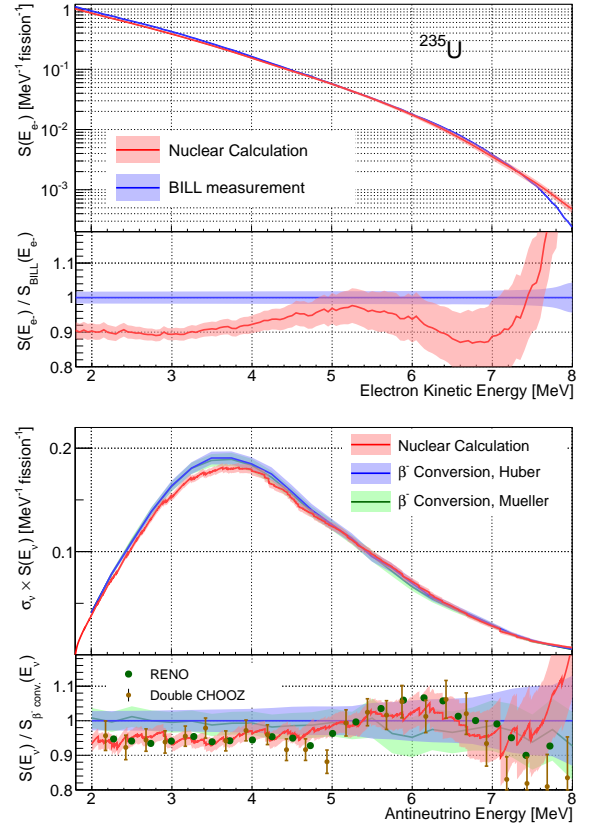


FIG. 1. Upper: The *ab initio* nuclear calculation of the cumulative  $\beta^-$  energy spectrum per fission of  ${}^{235}\text{U}$  exposed to thermal neutrons (red), including  $1\text{-}\sigma$  uncertainties due to fission yields and branching fractions. The measured  $\beta^-$  spectrum from [6] is included for reference (blue). Lower: The corresponding  $\bar{\nu}_e$  spectrum per fission in a nominal reactor weighted by the inverse beta decay cross section (red), compared with that obtained by the  $\beta^-$  conversion method (blue [12], green [11]). See text for discussion of uncertainties. Measurements of the positron spectra (green [22], brown [23]) are similar to the *ab initio* calculation, assuming the approximate relation  $E_{\bar{\nu}} \simeq E_{e^+} + 0.8$  MeV.

The significant differences between the calculation and BILL measurements are generally attributed to systematic uncertainties in the *ab initio* calculation. The  $1\text{-}\sigma$  uncertainty bands presented here include only the stated uncertainties in the cumulative yields and branching fractions. Three additional systematic uncertainties are prominent but not included: data missing from nuclear databases, biased branching fractions, and beta decay spectral shape corrections.

*Missing Data:* It is possible that the ENDF/B tabulated fission yields lack data on rare and very short lived isotopes in regions far from nuclear stability. In [16] it was argued that this missing data would favor higher-energy decays. For the known fission daughters,  $\sim 6\%$  of

the yielded isotopes have no measured beta decay information. Both of these effects result in an underprediction of the spectrum at all energies.

**Biased Branching Fractions:** The branch information for known isotopes may be incomplete or biased. For example the pandemonium effect can cause a systematic bias enhancing branching fractions at higher energies relative to those at lower energies [24]. Such a bias would cause an underprediction of the spectrum at low energies and an overprediction at high energies.

**Shape Corrections:** The beta decay spectra of each branch may vary from the allowed shape depending on the nuclear matrix elements connecting initial and final states. In general these corrections are small for allowed or slightly forbidden decays, but can be more significant for those decays involving a large  $\Delta J$  or cancellations between matrix elements. In [13] it was shown that  $\sim 25\%$  of known reactor  $\bar{\nu}_e$  decay branches are forbidden, and that shape corrections could in principle impact the  $\beta^-$  conversion method.

These systematic uncertainties are difficult to quantify and do hinder the absolute prediction of the  $\bar{\nu}_e$  rate and spectrum from a reactor. To correctly model and incorporate all of these uncertainties requires an extensive study not considered for this manuscript. Instead here we focus on two characteristics of the calculation which appear robust to these uncertainties. First, the combined distribution of beta decay branches predicts a bump in the antineutrino spectrum from 5 to 7 MeV. Second, the Coulomb corrections introduce detailed structure to the  $\bar{\nu}_e$  spectrum that is not reflected in the corresponding  $\beta^-$  spectrum.

### SPECTRAL SHAPE IN 5–7 MEV

Recent measurements present a  $\sim 10\%$  excess in the positron spectrum from inverse beta decay in the region of  $E_{e^+}=4\text{--}6$  MeV ( $E_{\bar{\nu}}=5\text{--}7$  MeV), similar to the *ab initio* calculation. In this region, the spectral shape is dominated by eight prominent decay branches which contribute 42% of the calculated rate. All eight branches are transitions between the ground states of the initial and final isotopes, and all are first forbidden non-unique decays. The remaining  $\sim 1100$  decay branches each contribute at most 2% of the total rate, and individually have little influence on the spectral shape. Fig. 2 shows the *ab initio* prediction broken into the eight major branches and the remaining minor branches. Table I summarizes these prominent decay branches.

The impact of each unquantified systematic uncertainty on this spectral feature can be examined. Contributions from missing nuclear data could add additional decay branches in this region, increasing the overall normalization and difference from the  $\beta^-$  conversion model. To remove the bump-like shape, it would require that

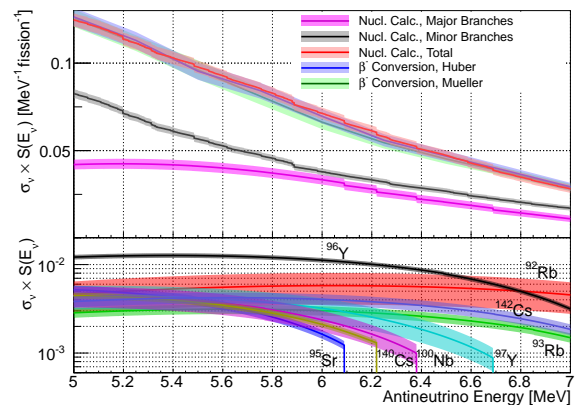


FIG. 2. Upper: The calculated reactor  $\bar{\nu}_e$  spectrum per fission in a nominal nuclear power reactor multiplied by the cross section for inverse beta decay (red), in the 5–7 MeV region. The eight most prominent decay branches in this region provide 42% of the total counts (magenta), and combine to produce a bump relative to the  $\beta^-$  conversion method (blue [12], green [11]). The remaining  $>1100$  decay branches each provide less than 2% of the total rate in this region, and combined provide a smooth shape (black). Lower: Individual spectra from the eight most prominent branches. Uncertainties are the same as for Fig 1.

Isotope	Q[MeV]	$t_{1/2}$ [s]	$\log(ft)$	Decay Type	$N[\%]$	$\sigma_N[\%]$
$^{96}\text{Y}$	7.103	5.34	5.59	$0^- \rightarrow 0^+$	13.6	0.8
$^{92}\text{Rb}$	8.095	4.48	5.75	$0^- \rightarrow 0^+$	7.4	2.9
$^{142}\text{Cs}$	7.308	1.68	5.59	$0^- \rightarrow 0^+$	5.0	0.7
$^{97}\text{Y}$	6.689	3.75	5.70	$1/2^- \rightarrow 1/2^+$	3.8	1.1
$^{93}\text{Rb}$	7.466	5.84	6.14	$5/2^- \rightarrow 5/2^+$	3.7	0.5
$^{100}\text{Nb}$	6.381	1.5	5.1	$1^+ \rightarrow 0^-$	3.0	0.8
$^{140}\text{Cs}$	6.220	63.7	7.05	$1^- \rightarrow 0^+$	2.7	0.2
$^{95}\text{Sr}$	6.090	23.9	6.16	$1/2^+ \rightarrow 1/2^-$	2.6	0.3

TABLE I. Most prominent beta decay branches in the region of  $E_{\bar{\nu}}=5\text{--}7$  MeV. The table presents the decay parent, end-point energy, half-life, and decay  $ft$  value. The decay type describes the parent and daughter states. The moderate  $ft$  values and lack of significant change of  $J^\pi$  suggest that all but possibly  $^{140}\text{Cs}$  decay with allowed spectral shapes. The rate each branch contributes to the total between 5–7 MeV is  $N$ , accounting for the inverse beta decay cross section. The  $1\text{-}\sigma$  uncertainty due to the fission yield and branching fraction is  $\sigma_N$ .

the additional branches have a particular distribution of endpoints just below and just above the excess. While possible, this seems contrived. For the eight prominent branches, six are  $0^-$  decays. These decays are not expected to have any significant deviation from allowed shapes. The  $ft$  values are mostly in the 5 to 6 range, consistent with allowed shapes. Only  $^{140}\text{Cs}$  has a large  $ft$  value and decay type consistent with a possible forbidden shape correction. Since this isotope contributes only 2.7% of the rate, the resulting correction should be

small. Forbidden shape corrections on the numerous minor branches can only negligibly impact the overall structure, although a cumulative effect could slightly impact the normalization and slope. The current uncertainty band includes the stated uncertainties on the branching fractions. Biases such as the pandemonium effect would need to be significantly larger than these uncertainties on the eight major branches in order to remove the bump-like shape. Pandemonium corrections on the large number of minor branches could slightly reduce the total normalization and change the slope in this region. In particular,  $^{92}\text{Rb}$  suffers from significant uncertainty in the branching fraction to the ground state. Our calculation used a branching fraction of  $51 \pm 18\%$  from [25]. In [26] it was changed to  $95 \pm 0.7\%$  to correct for a corresponding overestimation of branching fractions for known excited levels. Recent measurements suggest this may actually be due to unknown excited levels, providing a preliminary result of  $74\%$  [27]. Awaiting a definitive measurement, we retain the older value and larger uncertainty. While these uncertainties could reasonably impact the normalization and slope of the spectrum in this region, the prediction of a bumped shape seems robust provided the tabulated data for these prominent branches is correct.

Fig. 1 includes the recently measured deviations in the positron spectrum from inverse beta decay [22, 23]. The relation  $E_{\bar{\nu}} \simeq E_{e^+} + 0.8 \text{ MeV}$  was used to approximate the ratio for  $\bar{\nu}_e$  energy. Normalization was adjusted to provide a comparison of only spectral shape. Each experimental spectrum includes percent-level systematic effects from detector resolution and nonlinearity not present in the calculation, providing only an illustrative comparison. Given these assumptions and the model uncertainties already discussed, the overall agreement between the data and *ab initio* calculation is surprising.

### DETAILED SPECTRAL SUBSTRUCTURE

The *ab initio* calculated spectrum shows detailed substructure due to beta decay Coulomb corrections. The effect of the Coulomb correction on a single decay branch can be seen as the sharp discontinuity at the endpoint of the  $\bar{\nu}_e$  spectra. There is no corresponding detailed structure in the  $\beta^-$  spectrum since the Coulomb corrections impact the low-energy end of the electron spectrum. The substructure in the *ab initio* calculation is most apparent in the ratio relative to a smooth analytic approximation [28],

$$F(E_{\bar{\nu}}) = \exp\left(\sum_i \alpha_i E_{\bar{\nu}}^{i-1}\right). \quad (3)$$

A fit to the calculated spectrum provides  $\alpha = \{0.4739, 0.3877, -0.3619, 0.04972, -0.002991\}$ . A significant number of discontinuities are present with amplitudes of a few percent or greater, as shown in Fig. 3.

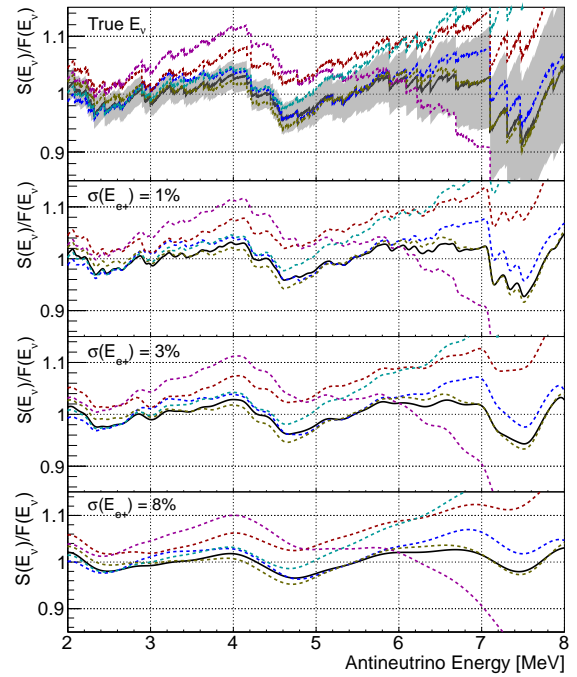


FIG. 3. Upper panel: The calculated  $\bar{\nu}_e$  energy spectrum from a nominal nuclear reactor (black line) divided by a smooth approximation [Eq. (3)], including the  $1\text{-}\sigma$  uncertainties due to the fission yields and branching fractions (grey band). Significant discontinuities are caused by the Coulomb correction to the spectra of prominent beta decays. Random variation of fission yields and branching fractions can alter the particular pattern (colored lines). Lower panels: The same spectra after accounting for detector resolution. The current generation of experiments with  $\sim 8\%$  resolution are sensitive to the larger variations. Future high-resolution experiments would detect significant substructure.

Systematic uncertainties in the *ab initio* calculation introduce variation in the specific pattern of this substructure. In alternative calculations, random gaussian fluctuations were applied to the yields and branching fractions according to the tabulated  $1\text{-}\sigma$  uncertainties. Parameters were not allowed to fluctuate to negative values, introducing a bias toward enhancing the overall spectrum. Fig. 3 shows five example spectra from these calculations.

The unquantified systematic uncertainties can also modify the substructure. Missing nuclear data would introduce additional isotopes and decay branches, thereby increasing the number of discontinuities. The pandemonium effect would slightly reduce the amplitude of discontinuities at high energies, and enhance those at low energies. Shape corrections can increase or decrease the amplitude of a particular discontinuity. While these uncertainties can make the exact pattern of substructure difficult to predict, it is clear that substructure of the scale shown will be present.

Current reactor  $\bar{\nu}_e$  experiments have sufficient resolu-

tion ( $6$  to  $8\% \times \sqrt{E_{e+}/1 \text{ MeV}}$ ) and statistical precision to be sensitive to these detailed spectral features. Fig. 3 demonstrates the spectral structure after accounting for detector resolution in the measurement of positrons from inverse beta decay. Measurements reaching percent-level resolution would reveal significant details of the nuclear processes occurring within a reactor. Once measured, the structure may also prove useful for calibration of future detectors. With further study it could possibly serve as a diagnostic for nuclear reactor operation. These features can pose an additional systematic uncertainty in measurements relying on the spectral shape. For example, proposed measurements of the neutrino mass hierarchy using reactor  $\bar{\nu}_e$  require detectors with an energy resolution of at least 3% [14, 15]. Given that the mass hierarchy presents itself as small differences in the high-frequency oscillatory pattern in the spectrum, the detailed spectral structure may complicate the measurement.

## DISCUSSION

While there are still significant uncertainties in *ab initio* calculation of the reactor  $\bar{\nu}_e$  energy spectrum, two specific characteristics are predicted. A spectral bump due to prominent beta decay branches in the 5–7 MeV region is similar to that seen in recent measurements. Dedicated studies of the fission yields and branching fractions of these prominent decays would help confirm the spectral shape in this region. The presence of this bump in both the calculated electron and antineutrino spectra suggests that the discrepancy may not be due to systematics of the  $\beta^-$  conversion method, but instead may be an artifact of the original  $\beta^-$  measurements.

Calculation can also predict the level of substructure in the  $\bar{\nu}_e$  energy spectrum from a reactor, but not the particular pattern. This may pose an additional challenge for measurements probing high-resolution features in the spectrum. Conversely, a high-resolution measurement of the reactor antineutrino spectrum could provide useful information for the modeling of nuclear fission within the reactor core.

These conclusions demonstrate the value of precise measurement of the  $\bar{\nu}_e$  energy spectra from nuclear reactors, reinforcing the conclusion of Ref. [13]. Research reactors could provide a model system (primarily  $^{235}\text{U}$ ) for comparison of measurement and calculation.

We would like to thank Richard Kadel for motivating this study, as well as Anna Hayes for assistance and for providing tabulated nuclear data. Critical discussions with Karsten Heeger, David Jaffe, and Petr Vogel helped elucidate this work. Brian Fujikawa and Herb Steiner gave very helpful suggestions during the preparation of this manuscript. This work was supported under DOE

OHEP DE-AC02-05CH11231 and DE-FG02-14ER42064.

\* dadwyer@lbl.gov

† thomas.langford@yale.edu

- [1] Y. Abe *et al.* (DOUBLE-CHOOZ Collaboration), Phys.Rev.Lett. **108**, 131801 (2012), arXiv:1112.6353 [hep-ex].
- [2] F. An *et al.* (DAYA-BAY Collaboration), Phys.Rev.Lett. **108**, 171803 (2012), arXiv:1203.1669 [hep-ex].
- [3] J. Ahn *et al.* (RENO collaboration), Phys.Rev.Lett. **108**, 191802 (2012), arXiv:1204.0626 [hep-ex].
- [4] F. An *et al.* (Daya Bay Collaboration), Phys.Rev.Lett. **112**, 061801 (2014), arXiv:1310.6732 [hep-ex].
- [5] S.-H. Seo (RENO Collaboration), (2013), arXiv:1312.4111 [physics.ins-det].
- [6] K. Schreckenbach, G. Colvin, W. Gelletly, and F. Von Feilitzsch, Phys.Lett. **B160**, 325 (1985).
- [7] F. Von Feilitzsch, A. Hahn, and K. Schreckenbach, Phys.Lett. **B118**, 162 (1982).
- [8] A. Hahn, K. Schreckenbach, G. Colvin, B. Krusche, W. Gelletly, *et al.*, Phys.Lett. **B218**, 365 (1989).
- [9] N. Haag, A. Gtlein, M. Hofmann, L. Oberauer, W. Potzel, *et al.*, Phys.Rev.Lett. **112**, 202501 (2014), arXiv:1312.5601 [nucl-ex].
- [10] R. Carter, F. Reines, J. Wagner, and M. Wyman, Phys.Rev. **113**, 280 (1959).
- [11] T. Mueller, D. Lhuillier, M. Fallot, A. Letourneau, S. Cormon, *et al.*, Phys.Rev. **C83**, 054615 (2011), arXiv:1101.2663 [hep-ex].
- [12] P. Huber, Phys.Rev. **C84**, 024617 (2011), arXiv:1106.0687 [hep-ph].
- [13] A. Hayes, J. Friar, G. Garvey, G. Jungman, and G. Jonkmans, Phys.Rev.Lett. **112**, 202501 (2014), arXiv:1309.4146 [nucl-th].
- [14] J. Learned, S. T. Dye, S. Pakvasa, and R. C. Svoboda, Phys.Rev. **D78**, 071302 (2008), arXiv:hep-ex/0612022 [hep-ex].
- [15] Y.-F. Li, J. Cao, Y. Wang, and L. Zhan, Phys.Rev. **D88**, 013008 (2013), arXiv:1303.6733 [hep-ex].
- [16] P. Vogel, G. Schenter, F. Mann, and R. Schenter, Phys.Rev. **C24**, 1543 (1981).
- [17] T. England and B. Rider, ENDF **349** (1992).
- [18] M. Chadwick *et al.*, Nucl.Data.Sheets **112**, 2887 (2011).
- [19] J. Tuli, NIM **A369**, 506 (1996).
- [20] G. Schenter and P. Vogel, Nucl.Sci.Eng. **83**, 393 (1983).
- [21] A. Sirlin, Phys.Rev. **D84**, 014021 (2011), arXiv:1105.2842 [hep-ph].
- [22] S. Seo *et al.* (RENO Collaboration), Presentation given at Neutrino2014 (2014).
- [23] Y. Abe *et al.* (Double Chooz Collaboration), (2014), arXiv:1406.7763 [hep-ex].
- [24] J. Hardy, L. Carraz, B. Jonson, and P. Hansen, Phys.Lett. **B71**, 307 (1977).
- [25] C. M. Baglin, Nucl.Data.Sheets **91**, 423 (2000).
- [26] C. M. Baglin, Nucl.Data.Sheets **113**, 2187 (2012).
- [27] A.-A. Zakari-Issoufou *et al.*, EPJ Web of Conferences **66**, 10019 (2014).
- [28] P. Vogel and J. Engel, Phys. Rev. D **39**, 3378 (1989).